Natural Resources Canada | Ressources naturelles Canada

CANADIAN GEOSCIENCE MAP 231

GEOLOGY

MONTRESOR RIVER AREA

Nunavut
parts of NTS 66-H and NTS 66-I

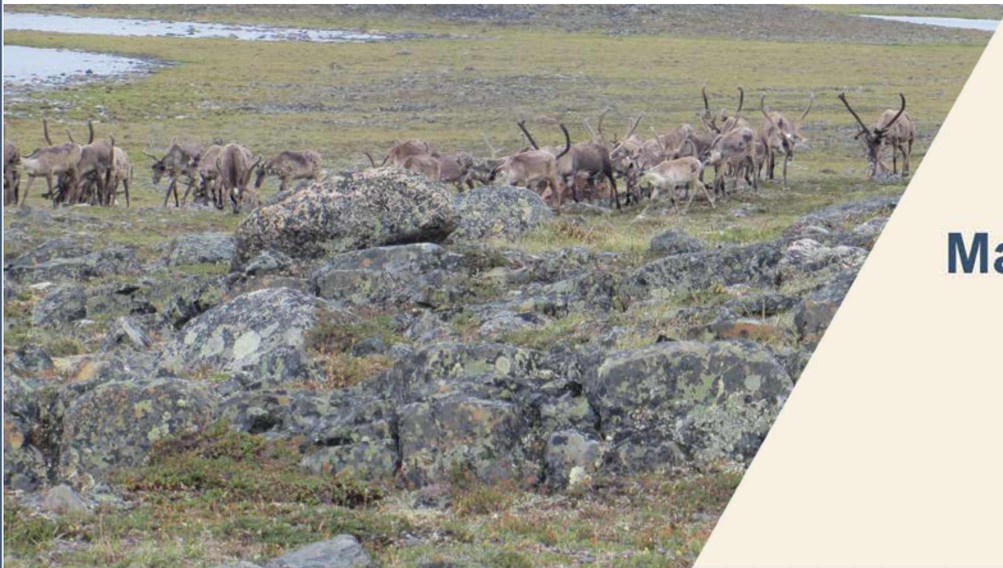

Map Information Document

Preliminary

Geological Survey of Canada
Canadian Geoscience Maps

2015

Canada

PUBLICATION

Map Number

Natural Resources Canada, Geological Survey of Canada
Canadian Geoscience Map 231 (Preliminary)

Title

Geology, Montresor River area, Nunavut, parts of NTS 66-H and NTS 66-I

Scale

1:100 000

Catalogue Information

Catalogue No. M183-1/231-2015E-PDF
ISBN 978-0-660-02703-6
doi:10.4095/296915

Copyright

Recommended Citation

Percival, J.A., Tschirhart, V., Davis, W.J., Berman, R.G., and Ford, A., 2015. Geology, Montresor River area, Nunavut, parts of NTS 66-H and NTS 66-I; Geological Survey of Canada, Canadian Geoscience Map 231 (preliminary), scale 1:100 000. doi:10.4095/296915

ABSTRACT

The Montresor River area (parts of NTS 66-H/13, 14, 15, 16, and NTS 66-I/1, 2, 3, 4, 5, 6, 7, 8), part of the Rae structural province, is underlain by granitic rocks of Archean (ca. 2.6 Ga) age and the Paleoproterozoic (<2.19 Ga) Montresor group of metasedimentary rocks. Quartzite, dolostone and metapelite of the lower Montresor group are structurally imbricated (D_1) with granitic gneisses and metamorphosed to the amphibolite facies. This structural footwall complex is separated from greenschist-facies rocks of the upper Montresor group by a detachment fault (D_2). A third set of structures including mylonites juxtaposes the basal footwall complex and surrounding granitoid rocks carrying concordant augen gneissic fabric. The Montresor syncline, outlined aeromagnetically by prominent magnetic siltstone beds, may be a D_4 structure. Previously unrecognized breccia and hydrothermally altered alkaline igneous rocks occur as a stratabound layer in the southwestern Montresor syncline and have elevated Cu, Ag, Au values.

RÉSUMÉ

La région de la rivière Montresor (parties des feuillets 66-H/13, 14, 15, 16 et 66-I/1, 2, 3, 4, 5, 6, 7, 8 du SNRC), située dans la province structurale de Rae, présente un sous-sol formé de roches granitiques de l'Archéen (env. 2,6 Ga) et de roches métasédimentaires du groupe de Montresor du Paléoprotérozoïque (<2,19 Ga). Les unités de quartzite, de dolomie et de métapélite du groupe de Montresor inférieur sont structuralement imbriquées (D_1) avec des gneiss granitiques et métamorphisées au faciès des amphibolites. Ce complexe de mur structural est séparé par une faille de décollement (D_2) des roches du groupe de Montresor supérieur, métamorphisées au faciès des schistes verts. Un troisième ensemble de structures, comprenant des mylonites, met en contact la partie basale du complexe de mur avec les roches granitoïdes environnantes, qui présentent des fabriques de gneiss œillé concordantes. Le synclinal de Montresor, mis en évidence dans les données aéromagnétiques par des lits de siltstone à forte signature magnétique, pourrait être une structure D_4. Dans la partie sud-ouest du pli synclinal de Montresor, des brèches et des roches ignées alcalines ayant subi une altération hydrothermale, non relevées jusque-là, forment une couche stratoïde renfermant des teneurs élevées en Cu, Ag et Au.

ABOUT THE MAP

General Information

Authors: J.A. Percival, V. Tschirhart, W.J. Davis, R.G. Berman, and A. Ford

Geology by J.A. Percival, V. Tschirhart, A. Ford, and C. Dziawa, 2012 and 2014

Geology conforms to Bedrock Data Model v. 1.1a

Geomatics by A. Ford

Cartography by A. Ford and E. Everett

Initiative of the Geological Survey of Canada, conducted under the auspices of the Rae project as part of Natural Resources Canada's Geo-mapping for Energy and Minerals (GEM-2) program

Logistical support provided by the Polar Continental Shelf Program as part of its mandate to promote scientific research in the Canadian north. PCSP 017-14

Map projection Universal Transverse Mercator, zone 14.
North American Datum 1983

Base map at the scale of 1:250 000 from Natural Resources Canada, with modifications.

Elevations in metres above mean sea level

Mean magnetic declination 2015, 2°50’W, increasing 1.7’ annually.
Readings vary from 1°07’W in the SW corner to 4°37’W in the NE corner of the map.

This map is not to be used for navigational purposes.

Title photograph: Siltstone of upper Montresor group (foreground) overlying quartz arenite and calc-silicate of the lower Montresor group (background), northeastern Montresor River area, Nunavut. Photograph by J.A. Percival. 2015-096

The Geological Survey of Canada welcomes corrections or additional information from users.

Data may include additional observations not portrayed on this map.
See documentation accompanying the data.

This publication is available for free download through
GEOSCAN (http://geoscan.nrcan.gc.ca/).

Preliminary publications in this series have not been scientifically edited.

Map Viewing Files

The published map is distributed as a Portable Document File (PDF), and may contain a subset of the overall geological data for legibility reasons at the publication scale.

Cartographic Representations Used on Map

This map utilizes ESRI Cartographic Representations in order to customize the display of standard GSC symbols for visual clarity on the PDF of the map only. The digital data still contains the original symbol from the standard GSC symbol set. The following legend features have Cartographic Representations applied:

Geochron sample

ABOUT THE GEOLOGY

Descriptive Notes

Introduction

The Montresor River area (part of Ian Calder Lake, NTS 66-I, NTS 66-H) is underlain by Precambrian rocks of the Rae structural province in central Nunavut, and includes two major geological features, the Montresor metasedimentary belt and part of the Amer mylonite zone. The area was initially mapped at 1:1M during Operation Northern Keewatin (Heywood, 1961) and subsequently at 1:250,000 (Frisch and Patterson, 1983; Frisch, 1992; 2000). Parts of the area were covered by a high-resolution aeromagnetic survey (Miles and Oneschuk, 2013) and GIS compilation including new information on archival samples (Harris et al., 2013). Geochronological results are reported for archival material from a regional transect (Davis et al., 2013) as well as for samples collected in 2012 (Davis et al., 2014). Results of a regional till survey are reported in McMartin et al. (2013). The present map results from compilation of existing information, augmented by integrated topical field work and geophysical interpretation in 2014 (Percival et al., 2015; Tschirhart et al., 2015).

Regional geology, structure, and metamorphism

Two main age groups are represented in the map area: Archean (ca. 2.6 Ga) granite and orthogneiss with sparse paragneiss and amphibolite enclaves; and Paleoproterozoic units including metasedimentary rocks of the Montresor belt (Frisch, 2000) and plutonic rocks. Archean granitoid rocks range in composition from tonalite to granodiorite and granite (Frisch, 2000). A K-feldspar porphyritic granodiorite representative of a regional-scale aeromagnetic low north of the Montresor belt yielded a U-Pb zircon age of 2589 ± 3 Ma (Davis et al., 2014). Within the map area these rocks range texturally from homogeneous and weakly foliated to augen gneissic, layered gneissic or mylonitic. They are generally metamorphosed in the amphibolite facies, except south of the Amer mylonite zone, where some rocks attained granulite facies (Fraser, 1988; Tella, 1994; Berman, 2010), dated at ca. 1.82 Ga locally (U-Pb monazite; Berman, 2010). At the regional scale, deformation and metamorphism of the Archean rocks is attributed to effects of both the ca. 2.35 Ga Arrowsmith and ca. 1.9–1.8 Ga Trans-Hudson orogeny (Berman et al., 2005; Berman, 2010; Berman et al., 2013a).

The Archean units have traditionally been considered to be depositional basement to the Montresor group, although no unconformity was observed (Frisch, 2000). Recent results support a more complex relationship among the Archean and Paleoproterozoic units (*see* Schematic tectonostratigraphic section, Fig. 1), including elements of the fold-thrust belt interpretation established in the Amer belt 50 km to the south (Patterson, 1986; Rainbird et al., 2010; Tschirhart et al., 2013; Pehrsson et al., 2013; Calhoun et al., 2014). The northeast end of the Montresor belt consists of a structural footwall complex made up of units including: augen gneiss (unit Āgg), quartz arenite and related arkose (unit PMq); chert, dolostone and related calc-silicates (unit PMc), as well as argillite and micaceous schist (unit PMp), the latter unit intruded by boudinaged sills of gabbro (locality 2; 2047 Ma; M.A. Hamilton, pers. comm., 2013) and foliated granodiorite. Assemblages in calc-silicate units including forsterite-diopside-tremolite indicate metamorphism at amphibolite facies. All units are transected by sparse narrow dykes of hornblende granodiorite, biotite granite and pegmatite. Contacts between augen gneiss and sedimentary units are characterized by deformation corridors of flaggy foliation, penetrative lineation, grain size reduction and obliteration of primary textures, and are interpreted as ductile fault zones (first phase of deformation, D_1). Map patterns of units and fault zones suggest polyphase structural imbrication of gneisses and sedimentary units. The metasedimentary rocks of the footwall complex are collectively referred to as the lower Montresor group. A structurally-bound quartzite from the Montresor footwall complex contains detrital zircons with a statistical peak of U-Pb SHRIMP ages at ca. 2190 Ma (locality 3; B. Davis, pers. comm., 2015), which together with the gabbro sill age, bracket deposition of the sedimentary units between 2190 and 2047 Ma. Lithologically, these units resemble regionally extensive quartzite, mudstone and dolostone strata exposed in the lower parts of the Amer and Ketyet River belts (Rainbird et al., 2010), informally known as Ps1 and Ps2 (Paleoproterozoic sedimentary units 1 and 2; Pehrsson et al., 2013). Structurally higher, in the core of the Montresor syncline, are weakly deformed and metamorphosed, fine-grained sandstone, siltstone, and calcareous sedimentary units informally referred to as the upper Montresor group. With U-Pb SHRIMP ages of ca. 3800–1938 Ma (locality 4; B. Davis, pers. comm., 2015), these units correspond to Ps3 units of the Amer and Ketyet River belts (Rainbird et al., 2010; Pehrsson et al., 2013). The nature of the boundary between the footwall complex and overlying upper Montresor units is best defined near the southwestern end of the belt. There, the footwall complex consists of muscovite-andalusite-sillimanite-garnet rich schist indicating middle-amphibolite facies conditions (3.3 kbar, 575°C) at 1861–1844 Ma (locality 6; Berman et al., 2015). Schistosity dips moderately northwest and is concordant with well-preserved bedding in the structurally overlying, weakly deformed sandstone and siltstone units of the upper Montresor group. Metamorphic assemblages in these fine-grained metasedimentary units include chlorite-muscovite-biotite and epidote-zoisite-clinozoisite-actinolite, defining middle greenschist-facies conditions, dated locally (locality 7) by metamorphic monazite at 1847 Ma (B. Davis, pers. comm., 2015). The interface between the upper and lower parts of the Montresor group is interpreted as a late- to post-metamorphic, low-angle extensional detachment fault (D_2) with vertical offset of several kilometres, to account for the missing upper greenschist- and lower amphibolite-facies rocks. Sedimentary units of the upper Montresor group include fine-grained, thinly laminated sandstone and siltstone, with sparse dolostone and calcareous sandstone (unit PMs). The siliciclastic units include laterally continuous beds with disseminated magnetite (unit PMsm) that form prominent aeromagnetic markers outlining a pair of doubly-plunging, open, upright synclines (D_4). In the southwestern syncline, a prominent aeromagnetic low corresponds to a stratabound unit of altered, brecciated igneous rocks (unit PMb). Pervasive hematite alteration within the unit suggests that oxidizing fluids may have been responsible for producing low magnetic susceptibilities. Observed over 4 kilometres of strike length, the zone can be extrapolated aeromagnetically for at least 50 km (Tschirhart et al., 2015; *see* Mineral Potential below).

The interpreted extensional fault separating the upper from the lower Montresor group is consistent with field observations of a metamorphic ‘gap’ between mid-greenschist and mid-amphibolite facies. However, the depositional relationship between the >2047 Ma lower Montresor and <1938 Ma upper Montresor is undefined. Possibilities include: 1) a disconformity encompassing a >109 million year depositional gap; 2) an unconformity between lower Montresor rocks, possibly deformed during the ca. 1.97 Ga Thelon orogeny (D_1-imbrication), and the upper Montresor sediments that contain 2.02–1.94 Ga detritus possibly derived from the Thelon orogen 300 km to the west. Although the stratigraphic nature of the contact cannot be defined in the Montresor belt, the correlative interface between sequences 2 and 3 is significant in the Amer and Ketyet River belts (Rainbird et al., 2010), where it is a disconformity or unconformity interpreted to reflect a change in tectonic setting from earlier extension to younger contraction and collision. In these belts, D_1 fold and thrust structures are bracketed between 1.93 and 1.83 Ga and probably close to 1.90 Ga (Pehrsson et al., 2013). This age could also apply to D_1 structures in the Montresor belt, which have been documented in the lower Montresor, and could also be present but unrecognized in the upper Montresor.

The southeastern boundary of the Montresor belt is exposed in locations northwest of the confluence of the Meadowbank and Back rivers. In that region, amphibolite-facies schist (unit PMp) of the lower Montresor Group is juxtaposed with augen gneiss across a moderately northwest-dipping mylonite zone (D_3) characterized by an intense, gently southwest-plunging stretching lineation. Rare kinematic indicators suggest a dextral, oblique sense of motion. Biotite granite and pegmatite dykes that transect schists northwest of the mylonite zone are deformed within the zone, where monazite within high-strain fabrics records U-Pb SHRIMP ages of 1850 Ma, (locality 8; B. Davis, pers. comm., 2015). Later muscovite-garnet granite and pegmatite dykes cut the mylonitic fabrics. The mylonite zone has not been observed at the northwestern margin of the belt but is included on the map for consistency. To the southeast, a moderately northwest-dipping ductile foliation characterizes augen gneisses in the 30 km-wide region toward the Amer mylonite zone. This zone has both ductile and brittle structures and experienced at least two periods of movement (Tella, 1994). The younger, brittle, dextral phase may have been as late as ca. 1700 Ma (Tella, op cit.) but the older, ductile phase could relate to events recognized in the Montresor belt. Specifically, a regional late-Trans-Hudsonian extensional event could relate the ca. 1.82 Ga granulite-facies metamorphism south of the Amer mylonite zone, to the ca. 1.85 Ga amphibolite and greenschist-facies metamorphism in the Montresor belt, through exhumation of a core complex accomplished by northwest-directed detachment.

At least three generations of diabase dykes are evident on aeromagnetic maps. North-south-trending dykes appear to be limited to the region between the Amer and Chantrey fault zones and have been named the Intra-Amer-Chantrey (IAC) dykes. A locality sampled north of the Back River yielded no zircon or baddelyite. Rare northeast-trending dykes may represent part of the undated Duggan swarm (Buchan and Ernst, 2013). Although prominent aeromagnetic features, northwest-trending dykes of the 1267 Ma Mackenzie swarm are poorly exposed in the area. The area is characterized by widespread glacial till and esker deposits.

Mineral potential

A single showing of copper and arsenopyrite was previously reported from the northern margin of the Montresor belt (Frisch, 2000). Several samples were assayed from the altered, brecciated zone (unit PMb) located to the east of the showing and one breccia returned anomalous values of Cu (1600 ppm), Ag (1700 ppb), Au (24 ppb), Bi (8.9 ppm), Se (36 ppm), and Te (1.5 ppm) (Berman et al., 2015). The stratabound zone, approximately 500 m thick where observed on the southeastern limb of the Montresor syncline, can be traced as an aeromagnetic low around the southwestern end of the syncline, and magnetic forward modeling supports a synclinal cross-sectional shape (Tschirhart et al., in press). At the upper contact, sedimentary rocks are variably silicified, brecciated and epidote-veined. Igneous rocks within the zone are variably altered to hydrothermal assemblages including actinolite, biotite, K-feldspar and tourmaline, and epithermal overprints characterized by epidote, chlorite, hematite and quartz. Breccias range texturally from multiply fractured or sheared rocks of unidentified protolith, to quartz-cemented stockworks with angular epidote and/or hematite-rich fragments. Original bulk compositions are obscure as a result of alteration and brecciation but the least altered rocks appear to have been silica undersaturated, possibly in the range alkali basalt to syenite. A relatively unaltered syenite yielded zircons ranging in age from 2.7 to 2.0 Ga, interpreted as inherited xenocrysts (B. Davis, pers. comm., 2015). The youngest zircon (2.0 Ga) represents a maximum age for emplacement. Textural observations indicate that the processes of igneous emplacement, alteration and brecciation overlapped in time. Fragments of altered basalt occur as xenoliths in syenite, itself altered and brecciated. In one location, thin basaltic dykelets cut breccia with a network of extensional veinlets. In terms of potentially analogous mineralized environments, Cu-Ag-Au deposits of Eocene age in the southwestern U.S.A. may be relevant. There, varieties of breccia, vein, epithermal and disseminated mineralization styles were deposited from oxidizing, low-sulphidation, Te-, Se-bearing fluids associated with alkaline magmatism in a regional extensional setting (e.g. Kelley and Ludington, 2002; Sillitoe, 2002; Sillitoe and Hedenquist, 2003; Richards, 2009; Colgan et al., 2014). Based on this analogy, the area may have potential for low grade, high-tonnage Cu-Ag-Au mineralization in a variety of mineralization styles.

References

Berman, R.G., 2010. Metamorphic map of the western Churchill Province, Canada; Geological Survey of Canada, Open File 5279, 3 sheets, 1:2 500 000 scale, + 49 p. report. doi:10.4095/287320

Berman, R.G., Nadeau, L., Percival, J.A., Harris, J., Girard, É., Whalen, J.B., Davis. W.J., Kellett, D., Jefferson, C.W., Camacho, A., and Bethune, K., 2015. Geo-Mapping Frontiers' Chantrey project: bedrock geology and multidisciplinary supporting data of a 550 kilometre transect across the Thelon tectonic zone, Queen Maud block, and adjacent Rae craton; Geological Survey of Canada, Open File 7698, 1 .zip file. doi:10.4095/296202

Berman, R.G., Pehrsson, S., Davis, W.J., Ryan, J.J., Qui, H., and Ashton, K.E., 2013a. The Arrowsmith orogeny: geochronological and thermobarometric constraints on its extent and tectonic setting in the Rae craton, with implications for pre-Nuna supercontinent reconstruction; Precambrian Research, vol. 232, p. 44–69.

Berman, R.G., Percival, J.A., Harris, J.R., Davis, W.J., McCurdy, M., Normandeau, P., Case, G., Nadeau, L., Hillary, E.M., Girard, E., Jefferson, C.W., Kellett, D., Camacho, A., Bethune, K.M., Pehrsson, S., and Hunt, P., 2013b. Geo-Mapping Frontiers' Chantrey project: Reconnaissance geology and economic potential of a transect across the Thelon tectonic zone, Queen Maud block, and adjacent Rae craton; Geological Survey of Canada, Open File 7394, 1 poster. doi:10.4095/292588

Berman, R.G., Sanborn-Barrie, M., Stern, R.A., and Carson, C.J., 2005. Tectonometamorphism at ca. 2.35 and 1.85 Ga in the Rae domain, western Churchill Province, Nunavut, Canada: insights from structural, metamorphic and in situ geochronological analysis of the southwestern Committee Bay belt; Canadian Mineralogist, vol. 43, p. 409–442.

Buchan, K.L. and Ernst, R.E., 2013. Diabase dyke swarms of Nunavut, Northwest Territories and Yukon, Canada; Geological Survey of Canada, Open File 7464. doi:10.4095/293149

Calhoun, L., White, J.C., Jefferson, C.W., Patterson, J., and Tschirhart, V. 2014. Integrated geodatabase study of the complexly deformed U-hosting Paleoproterozoic Amer Group, Nunavut; Geological Survey of Canada, Scientific Presentation 19, 1 ppt file. doi:10.4095/293108

Colgan, J.P., Henry, C.D., and John, D.A., 2014. Evidence for large-magnitude, post-Eocene extension in the northern Shoshone Range, Nevada, and its implications for the structural setting of Carlin-type gold deposits in the lower plate of the Roberts Mountain Allochthon; Economic Geology, vol. 109, p. 1843–1862.

Davis, W.J., Berman, R.G., and MacKinnon, A., 2013. U-Pb geochronology of archival rock samples from the Queen Maud Block, Thelon Tectonic Zone and Rae Craton, Kitikmeot region, Nunavut, Canada; Geological Survey of Canada, Open File 7409. doi:10.4095/292663

Davis, W.J., Berman, R.G., Nadeau, L., and Percival, J.A., 2014. U-Pb zircon geochronology of a transect across the Thelon Tectonic Zone, Queen Maud region, and adjacent Rae craton, Kitikmeot Region, Nunavut, Canada. Geological Survey of Canada Open File 7652, 1 .zip file. doi:10.4095/295177

Fraser, J.A., 1988. Geology of the Woodburn Lake map area, District of Keewatin; Geological Survey of Canada, Paper 87-11.

Frisch, T., 1992. Geology, Ian Calder Lake, District of Keewatin, Northwest Territories; Geological Survey of Canada, Map 1780A, scale 1:250 000. doi:10.4095/183920

Frisch, T., 2000. Precambrian geology of Ian Calder Lake, Cape Barclay, and part of Darby Lake map areas, south-central Nunavut; Geological Survey of Canada, Bulletin 542, 51 pages (2 sheets).

Frisch, T. and Patterson, J.G., 1983. Preliminary Account of the Geology of the Montresor River area, District of Keewatin; *in* Current Research, Part A / Recherches en cours, Partie A; Geological Survey of Canada, Paper 83-1A, p. 103–108.

Harris, J.R., Hillary, E.M., Percival, J.A., Buller, G., Buenviaje, R., Bazor, D., Baer, S., Kiessling, G.M., Pehrsson, S.J., Davis, W., Berman, R.G., Wodicka, N., Beauchemin, M., Coyne, M., and Therriault, A.M., 2013. Geo-mapping Frontiers: Updated information on the regions covered by Operations Baker, Bathurst, Keewatin, Northern Keewatin, Thelon and Wager; Nunavut and Northwest Territories: GIS components; Geological Survey of Canada, Open File 7434. doi:10.4095/292744

Heywood, W.W., 1961. Geological notes, northern District of Keewatin (parts of 56, 57, 66 and 67); Geological Survey of Canada, Paper 61-18, 9 p. doi:10.4095/101098

Kelley, K.D. and Ludington, S., 2002. Cripple Creek and other alkaline-related gold deposits in the southern Rocky Mountains, USA: influence of regional tectonics; Mineralium Deposita, vol. 37, Issue 1, p. 38–60.

McMartin, I., Berman, R.G., Normandeau, P.X., and Percival, J.A., 2013. Till composition of a transect across the Thelon tectonic zone, Queen Maud block, and adjacent Rae craton: results from the Geo-Mapping Frontiers' Chantrey project; Geological Survey of Canada, Open File 7418. doi:10.4095/292801

Miles, W. and Oneschuk, D., 2013. Northeastern Thelon - Garry Lake, NU, aeromagnetic compilation, parts of NTS 55, 65, 66 and 76, Nunavut; Geological Survey of Canada, Open File 7461. doi:10.4095/292809

Patterson, J.G., 1986. The Amer Belt: remnant of an Aphebian foreland fold and thrust belt; Canadian Journal of Earth Sciences, vol. 23, 2012–2023.

Pehrsson, S., Berman, R.G., and Davis, W.J., 2013. Paleoproterozoic orogenesis during Nuna aggregation: a case study of reworking of the Archean Rae craton, Woodburn Lake, Nunavut; Precambrian Research, vol. 232, p. 167–188.

Percival, J.A., Tschirhart, V., Ford, A., and Dziawa, C., 2015. Report of activities for geology and mineral potential of the Chantrey-Thelon Area: GEM-2 Montresor project; Geological Survey of Canada, Open File 7707, 12 p. doi:10.4095/295673

Rainbird, R.H., Davis, W.J., Pehrsson, S., Wodicka, N., Rayner, N., and Skulski, T., 2010. Early Paleoproterozoic supracrustal assemblages of the Rae domain, Nunavut, Canada: intracratonic basin development during supercontinent break-up and assembly; Precambrian Research, vol. 181, p. 167–186.

Richards, J.P., 2009. Postsubduction Cu-Au and epithermal Au deposits: Products of remelting of subduction-modified lithosphere; Geology, vol. 37, p. 247–250.

Sillitoe, R.H., 2002. Some metallogenic features of gold and copper deposits related to alkaline rocks and consequences for exploration; Mineralium Deposita, vol. 37, Issue 1, p. 4–13.

Sillitoe, R.H. and Hedenquist, J.W., 2003. Linkages between volcanotectonic settings, ore-fluid compositions, and epithermal precious metal deposits; Society of Economic Geologists Special Publication 10, pp. 315–343.

Tella, S., 1994. Geology, Amer Lake (66H), Deep Rose Lake (66G) and parts of Pelly Lake (66F), District of Keewatin, Northwest Territories, Open File 2969, scale 1:250 000. doi:10.4095/194789

Tschirhart, V., Morris, W.A., Jefferson, C.W., Keating, P., White, J.C., and Calhoun, L., 2013. 3D geophysical inversions of the north-east Amer Belt and their relationship to the geologic structure; Geophysical Prospecting, 61, 547–560. doi: 10.1111/j.1365-2478.2012.01098.x

Tschirhart, V., Percival, J.A., and Jefferson, C.W., 2015. Geophysical models of the Montresor metasedimentary belt and its environs, central Nunavut, Canada; Canadian Journal of Earth Sciences, Volume 52, Number 10, p. 833–845.

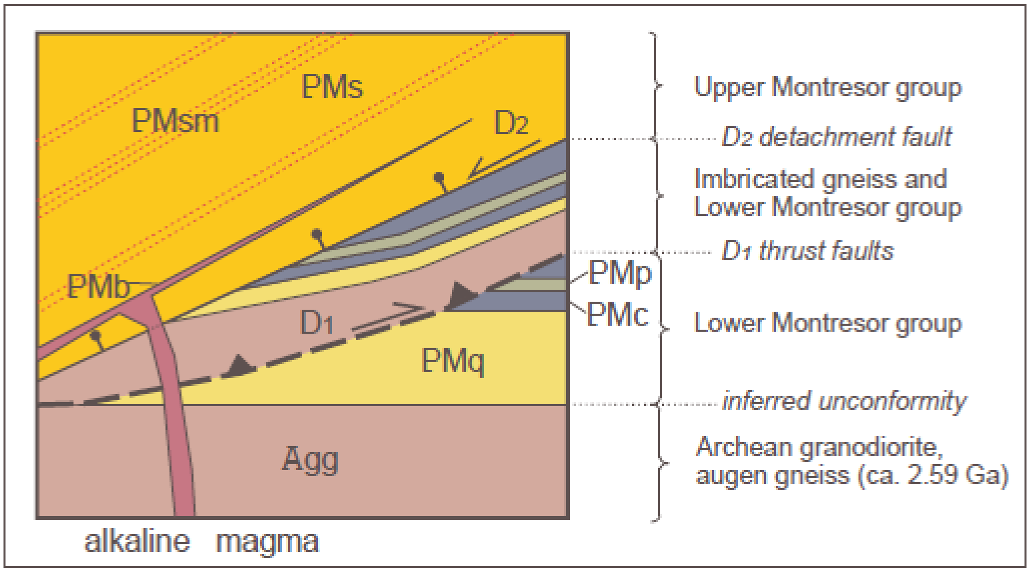

Figure 1. Schematic tectonostratigraphic section illustrating interpreted relationships among Archean and Paleoproterozoic units, and two generations of Paleoproterozoic structures in the Montresor belt.

No.	Unit	Sample Number	Age (Ma)	Error (Ma)	Method	Mineral	Interpretation	Significance	Reference
1	Agg	12PBA-23A1	2589	3	U-Pb SHRIMP	Zircon	Igneous crystallization age	Age of lithological unit Agg	1
2	gabbro sill	12PBA-B17E	2047	13	U-Pb TIMS	Zircon	Igneous crystallization age	Minimum depositional age for PMp	4
3	PMq	14PBA-29A1	<2190	-	U-Pb SHRIMP	Zircon	Youngest detrital zircon age	Maximum depositional age for PMq	3
4	PMs	12PBA-B19A	<1938	-	U-Pb SHRIMP	Zircon	Youngest detrital zircon age	Maximum depositional age for PMs	3
5	PMb	14PBA-102D	<2000	-	U-Pb SHRIMP	Zircon	Inheritance age	Maximum cystallization age for PMb syenite	3
6	PMp	12PBA-27A	1861	7	U-Pb SHRIMP	Monazite	Metamorphic crystallization age	Age of regional amphibolite-facies metamorphism	2
6	PMp	12PBA-27A	1844	6	U-Pb SHRIMP	Monazite	Metamorphic crystallization age	Age of regional amphibolite-facies metamorphism	2
7	PMs	14PBA-43	1847	15	U-Pb SHRIMP	Monazite	Metamorphic crystallization age	Age of regional greenschist-facies metamorphism	
8	Agg	14PBA-74A	1850	5	U-Pb SHRIMP	Monazite	Metamorphic crystallization age	D3 shear zone age	

Table 1. Summary table showing results of U-Pb age determinations and constraints for units and metamorphic events. Localities are numbered on the map face. References: 1 - Davis et al., 2014; 2 - Berman et al., 2015; 3 - Davis and Percival, unpublished data; 4 - Hamilton and Percival, unpublished data.

Author Contact

Questions, suggestions, and comments regarding the geological information contained in the data sets should be addressed to:

J.A. Percival
Geological Survey of Canada
601 Booth Street
Ottawa ON
K1A 0E8
John.Percival@canada.ca

Coordinate System

Projection: Universal Transverse Mercator
Units: metres

Zone: 14
Horizontal Datum: NAD83
Vertical Datum: mean sea level

Bounding Coordinates

Western longitude: 96°10’00”W
Eastern longitude: 115°30’00”W
Northern latitude: 63°30’00”N
Southern latitude: 65°50’00”N

Data Model Information

Bedrock

Geological Dataset accompanying this publication complies with the GSC’s Project Bedrock Schema. A short text describing the feature classes, tables and attributes is currently under review and will be made available for download shortly.